Nuclear Materials and Energy 12 (2017) 1184–1188

Contents lists available at ScienceDirect

Nuclear Materials and Energy

journal homepage: www.elsevier.com/locate/nme

High pulse number transient heat loads on beryllium

B. Spilker*, J. Linke, Th. Loewenhoff, G. Pintsuk, M. Wirtz

Forschungszentrum Jülich GmbH, Institut für Energie- und Klimaforschung, 52425 Jülich, Germany

ARTICLE INFO

Article history:
Received 30 June 2016
Revised 24 November 2016
Accepted 30 November 2016
Available online 27 December 2016

Keywords:
ELMs
Plasma facing materials
Beryllium
First wall
ITER
High heat flux testing
High pulse number

ABSTRACT

The experimental fusion reactor ITER will apply beryllium as first wall armor material. In present fusion experiments, e.g. ASDEX Upgrade, it has been detected that up to 25% of the plasma energy loss is deposited in non divertor regions during edge localized mode (ELM) events. Therefore, the impact of transient heating events on beryllium needs to be investigated to reliably predict the performance of the beryllium armor tiles under ITER operational conditions. In the present experiments, the electron beam facility JUDITH 2 was used to exert transient heat pulses with power densities of 0.14–1.0 GW m^{-2}, as they can be expected for mitigated Type 1 ELMs in ITER, pulse durations in the range of 0.08–1.0 ms, and a number of pulses in the range of 10^3–10^7 on S-65 beryllium specimens that were brazed on an actively cooled copper structure. Thereby, a strong drop of the melting threshold was discovered from a heat flux factor F_{HF} = 22–25 MW m^{-2}s$^{0.5}$ for 10^2 pulses to F_{HF} < 12 MW m^{-2}s$^{0.5}$ for 10^3 pulses. However, a saturation of the thermally induced damage was observed for $F_{HF} \leq 9$ MW m^{-2}s$^{0.5}$ after 10^5 pulses. This result indicated a promising performance of beryllium under a high number of transient heat pulses in ITER. Nevertheless, the synergistic effects between thermal loads, particle loads, and neutron irradiation might affect the saturation threshold and need to be investigated in future studies.

1. Introduction

Beryllium will be applied as plasma facing material (PFM) at the first wall (FW) in ITER, covering the major fraction of the inner surface of the vacuum vessel. The divertor, responsible for the main power exhaust, will be armored with tungsten as PFM. During the operation of ITER, the FW will be subjected to a variety of heat and particle loads. The edge localized mode (ELM) events during H-mode plasma operation deposit power densities of up to 1 GW m^{-2} on the PFMs and occur with a frequency f_{ELM} of several Hz, depending on the ELM mitigation scenario. The expected ELM frequencies of 3–5 Hz [1] translate to more than 10^7 ELM events during the lifetime of ITER. Accordingly, the beryllium armor will accumulate the induced surface damages throughout the entire operational time of ITER, since only the divertor is intended to be replaced after ~25,000 discharges [2]. Estimations of the beryllium erosion and damage accumulation are vital to identify possible threats for a high plasma performance originating from the condition of the FW.

Up to now, the highest number of transient heat pulses exerted on beryllium was 10^4 [3]. Depending on the absorbed energy density, surface morphology changes like roughening and cracking were observed. However, it remains unclear how this damage will develop with an increasing number of pulses. Earlier work investigated the response of beryllium at different base temperatures to different absorbed power densities for up to 10^2 pulses [4,5]. For tungsten, the drop of the damage threshold with an increasing number of pulses was reported in [6].

In the present work, ITER qualified S-65 grade beryllium specimens were subjected to as much as 10^7 transient heat pulses with absorbed power densities L_{abs} in the range of 0.14–1.0 GW m^{-2} and pulse durations t in the range of 0.08–1.0 ms. The pulse duration of 0.08 ms in combination with a repetition frequency of 67 Hz was chosen for comparison with the modelling of the ELM heat flux deposition on the ITER main chamber wall in [7]. Furthermore, the pulse durations of 0.48 ms and 1.0 ms were chosen to enable a direct comparability of the results to earlier experiments performed at the JUDITH 1 and JUDITH 2 electron beam facilities. Within this work, JUDITH 2 was used to apply ELM-like heat loads using the beam guidance method that is described in [8]. The generated results provide insight into the long-term development of the beryllium armor surface condition in ITER.

* Corresponding author.
E-mail address: b.spilker@fz-juelich.de (B. Spilker).

http://dx.doi.org/10.1016/j.nme.2016.11.032

2. Experimental set-up

2.1. Fabrication of the actively cooled Be-Cu component

The transient heat load experiments performed in [3,4] used passive, inertial cooling. The pulse repetition frequency of 0.5 Hz was sufficiently low to keep the specimen at a constant base temperature throughout the loading. However, a high number of pulses required higher repetition frequencies than 0.5 Hz to decrease the experimental time to an acceptable level. Therefore, an actively cooled Be-Cu component was fabricated to allow the removal of the higher average energy influx. The Be-Cu component consisted of three S-65 grade beryllium specimens (for further material details, see [4]) with a size of $12 \times 12 \times 10\,mm^3$ and a polished top surface (1 µm diamond particle suspension). The examined S-65 beryllium material was characterized by a low beryllium oxide content of 0.6 wt% and a grain size of 13 µm (circular equivalent diameter). The specimens were brazed onto a copper structure, comparable to the copper block used in [8].

The brazing process was performed in the electron beam facility JUDITH 1, since it allows the handling of toxic beryllium at elevated temperatures. A silver-based brazing material containing 28 wt% Cu, 2 wt% Ge, and 0.3 wt% Co with a thickness of 100 µm was used to create a stable thermal contact between the beryllium specimen and the copper heat sink structure. This study solely focused on the effects at the loaded beryllium surface. The brazing process and the copper block were introduced for an efficient heat removal during the experiment, not to create a detailed mock-up prototype of the first wall design in ITER. Therefore, the characteristics of the Be-Cu joint were not considered in this work.

Without active cooling of the copper structure, the assembly was slowly heated by increasing the current of the electron beam. The temperature was measured with thermocouples located 1 mm below the bottom of the brazing pool in the copper structure. As soon as the temperature reached 830 °C, the beam current was adjusted and the temperature of the assembly was kept constant for three minutes. After that, the beam was switched off and the brazed Be-Cu component was cooled down to room temperature.

Subsequently, an energy dispersive X-ray spectroscopy (EDX) investigation was performed on the brazed beryllium specimen. Thereby, a significant amount of BeO was detected on the surface, despite the fact that the brazing was performed under JUDITH 1 vacuum conditions with $p = 10^{-4}$ mbar. To recover a well-defined, BeO free surface condition for the following electron beam tests, the beryllium surfaces were polished again with a 1 µm diamond particle suspension to a mirror finish (arithmetic mean roughness $R_a \approx 0.1\,\mu m$).

2.2. JUDITH 2 loading conditions

The flexible beam guidance method of JUDITH 2 allows creating transient heat loads with a minimum dwell time of 5 µs. Furthermore, to exert well defined ELM-relevant power densities, a precise measurement of the electron beam diameter was performed prior to the experiment [9]. Following the evaluation of the electron beam diameter, the optimum acceleration voltage was determined to be 40 kV for the generation of the desired power densities on the specimens. A Monte Carlo simulation using the CASINO software [10] was carried out in order to estimate the electron penetration depth in the experiment. In this simulation, 5000 electrons with a kinetic energy of 40 keV were perpendicularly impinging a flat surface of a beryllium block. The resulting energy deposition profile as well as the scattering cascade inside the material enabled the determination of the electron penetration depth of 18 µm and the electron absorption coefficient of $\varepsilon = 0.98$.

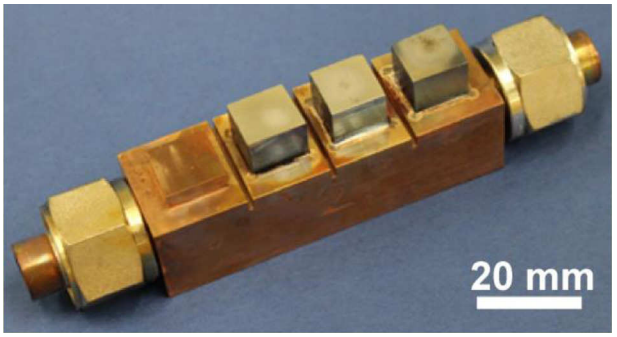

Fig. 1. Photograph of the brazed, actively cooled Be-Cu component (after testing). The copper tile on the left side provides an area used for the adjustment of the electron beam pattern and aiming procedures.

The beam pattern was designed to apply power densities of $L_{abs} = 0.14–1.0\,GW\,m^{-2}$ with pulse durations of $t = 0.08–1.0$ ms, which translate to heat flux factors ($F_{HF} = L_{abs} \times t^{0.5}$) in the range of $F_{HF} = 3–12\,MW\,m^{-2}s^{0.5}$, and repetition frequencies of $f_{ELM} = 0.5–67$ Hz. At 25 Hz and 67 Hz, the application of 10^6 and 10^7 pulses takes 11.11 h and 41.46 h of active beam time, respectively. To achieve the desired specimen base temperatures T_{base} of 250 °C and 400 °C, the active cooling system in JUDITH 2 was set to a water inlet temperature of 100 °C and a flowrate of 80 l/min was used. Additionally, the beam pattern was adjusted accordingly to provide a steady state heat load on the entire component that yielded the intended base temperature on the beryllium specimens. The steady state heat load did not cause any alteration of the polished surfaces of the beryllium specimens. Therefore, all detected damages were solely originating from the transient heat loading. Fig. 1 shows an image of a Be-Cu component after the testing in JUDITH 2.

The sample base temperature was controlled via an IR camera. Furthermore, the temperature and surface condition dependent emissivity was determined with a single polished beryllium specimen mounted on a thermocouple prior to the experiment. With the generated data, a temperature dependent correction field was established within the view of the IR camera, which provided the respective emissivity values for the beryllium surfaces. Depending on the absorbed power density and the respective beam full width half maximum (FWHM, smaller for higher power densities), the homogeneously loaded circular area had a diameter of ~2–3 mm [9]. The base pressure of the experimental chamber in JUDITH 2 was about 3×10^{-4} mbar. The maximum surface temperatures reached during the experiment were calculated with the finite element method (FEM) model described in [11] adapted to the electron penetration depth in JUDITH 2. The model was based on a beryllium specimen with the same dimensions as in the experiment ($12 \times 12 \times 10\,mm^3$) and the heat flux was applied in the loaded volume defined by the loaded area with a size of $4 \times 4\,mm^2$ and the electron penetration depth of 18 µm.

Following the exposure in JUDITH 2, the samples were investigated by means of laser profilometry, scanning electron microscopy (SEM), and EDX.

3. Results and discussion

The damages induced by the various loading conditions are summarized in Fig. 2. In contrast to the experiments with tungsten in [8] and to the experiments with beryllium at 10^2 pulses in [4], the damage mapping categories “no damage” and “roughening” were not observed in the present experiments. The melting threshold after 10^2 pulses was determined in [4] to be in the range of $F_{HF} = 22–25\,MW\,m^{-2}s^{0.5}$. In the present experiments, localized melting was already observed at a significantly lower value

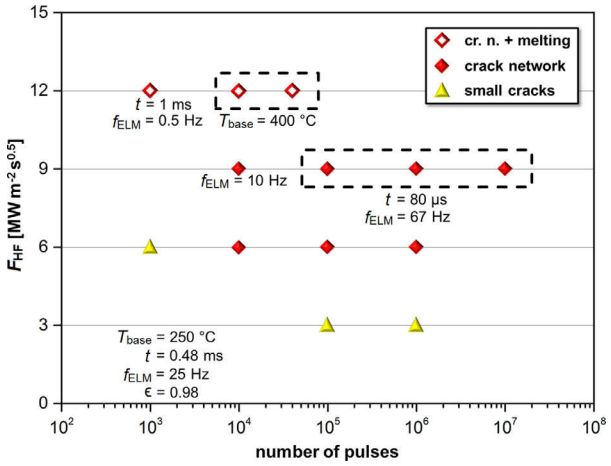

Fig. 2. Damage mapping for S-65 beryllium under transient heat loading. The conditions in the bottom left of the diagram (T_{base}: base temperature, t: pulse duration, f_{ELM}: ELM frequency, ε: electron absorption coefficient) apply to all data points unless marked differently. The conditions stated below dashed boxes apply for all data points within the boxes. The worst kind of damage found in the loaded area determined the damage category for the respective loading condition.

of $F_{HF} = 12\,MW\,m^{-2}s^{0.5}$ for $\geq 10^3$ pulses. This drop of the melting threshold can be explained by fatigue effects, e.g. the accumulation of plastic deformation and the disengagement of single grains at the surface. These effects became more pronounced with an increasing number of pulses. Thereby, the thermal conductivity in the affected layer decreased, as the results in [12] have shown for a surface damaged by comparable transient heat pulses. Moreover, the high number of pulses led to a significant roughening and change of the surface morphology. The average maximum surface temperature $T_{max} = 827\,°C$ for $F_{HF} = 12\,MW\,m^{-2}s^{0.5}$ and $t = 1$ ms at $T_{base} = 250\,°C$, determined by FEM calculations, did not exceed the beryllium melting temperature of 1287 °C.

Fig. 3(a) and (b) show overview images of the samples loaded with $F_{HF} = 12\,MW\,m^{-2}s^{0.5}$ for 10^3 and 4×10^4 pulses, respectively. The detailed view of the area loaded with $F_{HF} = 12\,MW\,m^{-2}s^{0.5}$ for 4×10^4 pulses in Fig. 3(c) revealed the melting of isolated particles on the surface as well as a noticeable BeO formation, as it was observed in earlier transient thermal load experiments [13]. The amount of beryllium oxide formed at the surface increased with T_{max} [4,14] as well as with the applied number of pulses (cf. Fig. 7). Resulting from the cyclic plastic deformation at the loaded surface, single beryllium grains or larger material fragments detached primarily at the grain boundaries and therefore became thermally isolated on the surface. These particles were prone to overheating and melting and defined the damage category "crack network + melting" ("cr. n. + melting" in Fig. 2), even though the loaded area was not entirely molten. The strong drop of the melting threshold in terms of F_{HF} in contrast to the results in [4] can be easily understood when the electron penetration depth is considered. The electron penetration depth for beryllium in JUDITH 1 with an acceleration voltage of 120 kV is 120 µm [4] compared to 18 µm for JUDITH 2 with an acceleration voltage of 40 kV, both determined by Monte Carlo simulations. Therefore, thermally isolated particles at the surface absorb a significantly larger fraction of the incident beam energy in JUDITH 2 experiments compared to JUDITH 1, where the energy absorption profile peaks at a depth of 64 µm below the surface [12]. In addition, the more volumetric load in JUDITH 1 did not cause as many loose grains or material fragments as the more surface affecting load in JUDITH 2.

For 10^3 pulses, the loading conditions of $F_{HF} = 12\,MW\,m^{-2}s^{0.5}$, $t = 1$ ms, $T_{base} = 250\,°C$, and $f_{ELM} = 0.5$ Hz were chosen to enable a direct comparability to the results in [4]. However, for $F_{HF} = 12\,MW\,m^{-2}s^{0.5}$ at 25 Hz repetition frequency, the average energy influx from the transient heat pulses was too high to keep the base temperature at $T_{base} = 250\,°C$. Therefore, it was decided to adjust the electron beam pattern to keep a constant base temperature of $T_{base} = 400\,°C$ for these loading conditions.

Considering the observed trends for the development of the cracking and melting thresholds to remain constant in the range of $T_{base} = 100$–$300\,°C$ in [4], it is assumed that the base temperature increase from 250 °C to 400 °C did not significantly alter the induced damages in terms of cracking and melting. The peak surface temperature for $F_{HF} = 12\,MW\,m^{-2}s^{0.5}$ and $t = 0.48$ ms at $T_{base} = 400\,°C$ was calculated to be $T_{max} = 950\,°C$ in contrast to $T_{max} = 827\,°C$ for the same F_{HF} value but $t = 1$ ms at $T_{base} = 250\,°C$.

As FEM calculations showed, the maximum temperature at the surface of the specimen decreases to the equilibrium base temperature with a maximum discrepancy of ~6% within 15 ms. Therefore, with $f_{ELM} = 67$ Hz and thus ~15 ms between two consecutive transient heat pulses, the impact of the interference between two consecutive pulses on the thermally induced damage is assumed to be negligible up to $f_{ELM} = 67$ Hz. The observed consistency of the damages induced by loading conditions with the same F_{HF} value but different repetition frequencies indicated that this assumption is reasonable for the present experiments.

The progression of the plastic deformation and roughening at the loaded surface was evaluated using the arithmetic mean roughness (R_a) value, plotted in Fig. 4. For $F_{HF} = 12\,MW\,m^{-2}s^{0.5}$, the R_a value strongly increased with an increasing number of pulses. For $F_{HF} = 9\,MW\,m^{-2}s^{0.5}$, the R_a value remained rather constant between 10^4 pulses and 10^6 pulses with a slight decrease at 10^7 pulses. This decrease can possibly be explained by the poor statistics since only one specimen per F_{HF} value and number of pulses was tested. Furthermore, due to the long timespan between the loading of the specimens and during the loading with 10^7 pulses (41.46 h at 67 Hz), a drift of the beam focus in JUDITH 2 could not be completely excluded. The beam diameter was measured prior to the entire experimental campaign but not prior to each loading condition due to operation time constraints. Therefore, aging processes of the cathode of the electron beam generator could affect the beam diameter during the experiments and vary the applied F_{HF}. An SEM image of the surface loaded with 10^7 pulses is provided in Fig. 5. The thermally induced crack network for this loading condition appeared to be similar to all other thermally induced crack networks for $F_{HF} = 6$–$9\,MW\,m^{-2}s^{0.5}$ and 10^5–10^6 pulses.

As the results in [11] show, the maximum temperature reached during transient heat loading with the same F_{HF} but different pulse durations tends to be lower for shorter pulses. Therefore, an FEM simulation with the same model as in [11], adapted to the electron penetration depth in JUDITH 2 of 18 µm, was performed for $F_{HF} = 9\,MW\,m^{-2}s^{0.5}$ and $t = 0.48$ ms as well as $t = 0.08$ ms. The maximum temperatures reached at the end of the transient heat pulses were $T_{max} = 661\,°C$ and $T_{max} = 635\,°C$ for $t = 0.48$ ms and $t = 0.08$ ms, respectively. The temperature difference of about 4% for $t = 0.48$ ms and $t = 0.08$ ms is rather small compared to the temperature difference of about 16% for $t = 5$ ms and $t = 1$ ms in [11]. Conclusively, the F_{HF} value can reasonably be addressed to compare transient heat pulses with durations in the range of 0.08–0.48 ms.

For $F_{HF} = 6\,MW\,m^{-2}s^{0.5}$, the R_a value slowly increased up to 10^5 pulses and seemed to saturate between 10^5 pulses and 10^6 pulses. The respective surfaces are shown in Fig. 6. The extent of the induced damage appeared similar for both loading conditions. However, EDX measurements revealed that the oxygen content on the surface loaded with 10^6 pulses of $F_{HF} = 6\,MW\,m^{-2}s^{0.5}$ is significantly higher, as it can be seen in Fig. 7. The calculated maximum temperature for this F_{HF} value at $T_{base} = 250\,°C$ was $T_{max} = 509\,°C$.

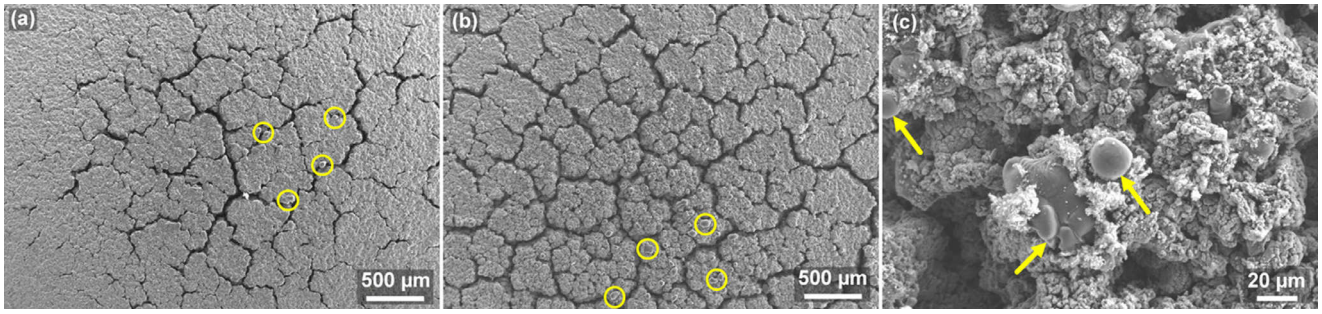

Fig. 3. SEM images of the areas loaded with $F_{HF} = 12$ MW m^{-2}s$^{0.5}$ and (a) 10^3 pulses, $T_{base} = 250$°C, $f_{ELM} = 0.5$ Hz, $t = 1$ ms, (b) 4×10^4 pulses, $T_{base} = 400$°C, $f_{ELM} = 25$ Hz, $t = 0.5$ ms. (c) Magnified view of (b). Molten droplets and areas are indicated with yellow circles and arrows.

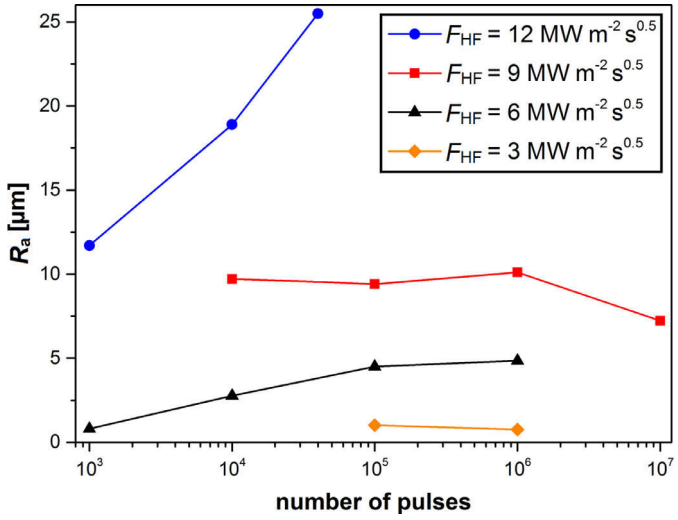

Fig. 4. Arithmetic mean roughness R_a measured via laser profilometry as a function of the number of applied transient thermal events.

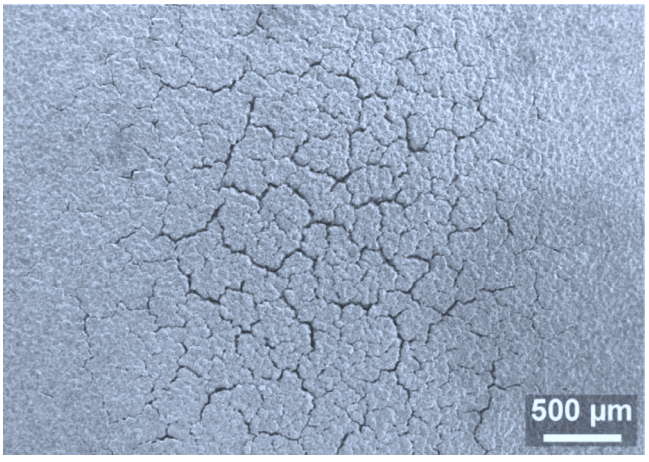

Fig. 5. SEM image of the area loaded with 10^7 pulses at $F_{HF} = 9$ MW m^{-2}s$^{0.5}$.

At this maximum temperature, the oxidation rate for beryllium was determined to be extremely low [15]. However, the strong oxygen getter capability of beryllium still absorbed the residual oxygen during the transient heat pulses from the JUDITH 2 vacuum chamber with an oxygen partial pressure of 6×10^{-5} mbar, as it was observed on previous transient heat load experiments with similar oxygen partial pressures [11]. The residual pressure in JUDITH 2 is about four orders of magnitude higher than the impurity partial pressure expected for the ITER vacuum chamber

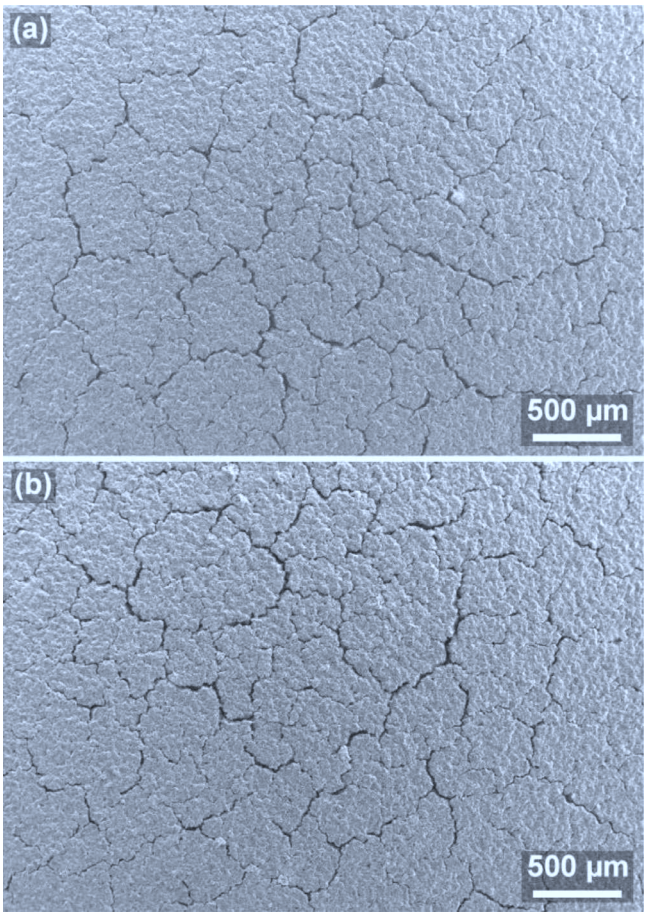

Fig. 6. SEM images of the areas loaded with $F_{HF} = 6$ MW m^{-2}s$^{0.5}$ and (a) 10^5 pulses, (b) 10^6 pulses.

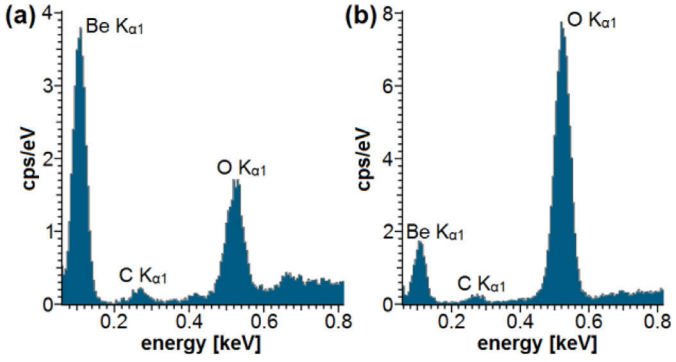

Fig. 7. EDX measurement of representative spots within the areas loaded with $F_{HF} = 6$ MW m^{-2}s$^{0.5}$ and (a) 10^5 pulses, (b) 10^6 pulses. Note the y scale difference.

[16]. Hence, the beryllium surface in ITER cannot absorb comparable amounts of oxygen during transients that induce maximum surface temperatures of $T_{max} \leq 509\,°C$ for up to 10^6 pulses.

For $F_{HF} = 3\,MW\,m^{-2}s^{0.5}$, only small, shallow, and isolated cracks accompanied by a slight roughening were observed on the loaded surface. Furthermore, the R_a value remained at about 1 µm for 10^5 pulses and 10^6 pulses. However, the detected surface modifications for $F_{HF} = 3\,MW\,m^{-2}s^{0.5}$ demonstrated that the damage threshold is located even below this F_{HF} value for 10^5 pulses.

The saturation of the R_a value in combination with the similar extent of the crack network at $F_{HF} \leq 9\,MW\,m^{-2}s^{0.5}$ from 10^4 pulses to 10^7 pulses indicated that there is a saturation threshold in terms of F_{HF}. If the transients in ITER that affect the FW remain below this threshold, the induced surface damage might saturate rather than accumulate with an increasing number of pulses. However, the interplay between particle loads, neutron irradiation, and transient heat loads in a thermonuclear reactor such as ITER could alter the damage behavior of beryllium and affect the saturation threshold.

4. Conclusions

The impact of a high number of transient heat pulses on beryllium was investigated using the flexible beam guidance of the electron beam facility JUDITH 2 on beryllium specimens that were brazed onto an actively cooled Cu heatsink. Thereby, it was discovered that the melting threshold of $F_{HF} = 22–25\,MW\,m^{-2}s^{0.5}$ for 10^2 pulses in earlier experiments at JUDITH 1 dropped to $F_{HF} = 9–12\,MW\,m^{-2}s^{0.5}$ for $\geq 10^3$ pulses in the present experiments. This drop can be explained by considering the electron penetration depth of only 18 µm in the present experiments compared to 120 µm in JUDITH 1. Particles with a poor thermal connection located at the surface were found on several locations throughout the loaded area as a result of the cyclic thermal expansion and contraction and the consequential plastic deformation, roughening, and cracking of the surface. These particles absorbed a high fraction of the incident beam energy due to the low electron penetration depth of JUDITH 2 and eventually melted, causing a significant drop of the melting threshold.

The transient heat loads originating from ELMs in ITER will be conveyed by plasma, which is absorbed by the beryllium surface and does not lead to a volumetric heating. Therefore, the lower electron penetration depth of JUDITH 2 provides a better experimental simulation of the transient heating of beryllium by ELMs in ITER than the more volumetric heating in JUDITH 1.

In conclusion, the cracking and melting thresholds in terms of F_{HF} dropped from 10^2 pulses to 10^3 pulses, which can be explained by a combination of the electron penetration depth for the different experiments at 10^2 pulses and 10^3 pulses and fatigue effects. Nevertheless, within the generated results, the cracking and melting thresholds remained constant from 10^3 pulses to 10^7 pulses for all tested loading conditions. Furthermore, the damage threshold for S-65 grade beryllium was determined to be located below $F_{HF} = 3\,MW\,m^{-2}s^{0.5}$ for 10^5 pulses. However, the damage induced at this F_{HF} value was rather slight with an arithmetic mean roughness of about 1 µm.

Lastly, the saturation of the R_a value from 10^4 pulses to 10^7 pulses at $F_{HF} \leq 9\,MW\,m^{-2}s^{0.5}$ in combination with the respective SEM images of the loaded areas indicated that there is a saturation threshold in terms of F_{HF} in the range of $F_{HF} = 9–12\,MW\,m^{-2}s^{0.5}$. Damages induced by transient heat loads with F_{HF} values below this threshold are expected to saturate after a certain number of pulses, while higher F_{HF} values will lead to damage accumulation with an increasing number of pulses. For ITER, this is a promising result since the possible ELM mitigation scenarios that pace ELMs to frequencies in the range of 33–67 Hz [7] could lead to more than 10^7 ELM events on the FW armor. The combination of the highest absorbed power density $L_{abs} \approx 1.0\,GW\,m^{-2}$ and a pulse duration $t \approx 0.08$ ms in [7] yields a heat flux factor of $F_{HF} \approx 9\,MW\,m^{-2}s^{0.5}$, which showed a saturation of the induced damage with an increasing number of pulses in the present work. If the ELMs in ITER do not exceed the F_{HF} saturation threshold found in the present work, the damage to the beryllium armor by ELMs might be limited. Further investigations are necessary to determine whether the synergistic effects between the particle loads (deuterium/tritium/seeding gases/impurities), neutron irradiation, and thermal loads affect the saturation threshold and accelerate the damage progression of beryllium.

Acknowledgments

The authors would like to kindly thank G. Knauf for her benevolent assistance in the preparation of the samples, Dr. E. Wessel for the performance of the SEM analyses and the Monte Carlo simulations, and K. Dominiczak as well as M. Lowis for the support of the JUDITH 2 experimental campaign.

References

[1] A. Loarte, et al., Fusion Energy 2010 (Proc. 23rd Int. Conf. Daejeon, 2010) (Vienna: IAEA) CD-ROM file [IAEA-CN-180] http://www-naweb.iaea.org/napc/physics/FEC/FEC2010/index.htm.
[2] R.A. Pitts, et al., J. Nucl. Mater. 438 (2013) S48–S56.
[3] M. Roedig, et al., J. Nucl. Mater. 417 (2011) 761–764.
[4] B. Spilker, et al., Phys. Scr. T167 (2016) 014024 (4pp).
[5] I.B. Kupriyanov, et al., Impact of high transient loads on beryllium damage, in: IEEE 25th Symposium on Fusion Engineering (SOFE), 2013, pp. 1–5.
[6] J. Linke, et al., Nucl. Fusion 51 (2011) 073017 (6pp).
[7] M. Kočan, et al., Modelling ELM heat flux deposition on the ITER main chamber wall, J. Nucl. Mat. 463 (2015) 709–713.
[8] Th. Loewenhoff, et al., Fusion Eng. Des. 87 (2012) 1201–1205.
[9] Th. Loewenhoff, et al., J. Nucl. Mater. 415 (2011) S51–S54.
[10] D. Drouin, et al., CASINO V2.42 – a fast and easy-to-use modeling tool for scanning electron microscopy and microanalysis user, Scanning 29 (2007) 92–101.
[11] B. Spilker, et al., Investigation of damages induced by ITER-relevant heat loads during massive gas injections on Beryllium, J. Nucl. Mater. Energy (2016). http://dx.doi.org/10.1016/j.nme.2016.06.006.
[12] S. Pestchanyi, et al., Simulation of be armour cracking under ITER-like transient heat loads, J. Nucl. Mater. Energy (2016). http://dx.doi.org/10.1016/j.nme.2016.06.007.
[13] B. Spilker, et al., Impact of the surface quality on the thermal shock performance of beryllium armor tiles for first wall applications, Fusion Eng. Des. 109–111 (2016) 1692–1696.
[14] B. Spilker, et al., Oxide segregation and melting behavior of transient heat load exposed beryllium, Nucl. Fusion 56 (2016) 106014 (9pp).
[15] G. Ervin Jr., T.L. Mackay, Catastrophic oxidation of beryllium metal, J. Nucl. Mat 12 (1) (1964) 30–39.
[16] R.J.H. Pearce, et al., ITER relevant outgassing and leakage from different types of in-vessel cabling, Fus. Eng. Des. 82 (5–14) (2007) 1294–1300.